# GENERALIZED Y-MATRIX OF ARBITRARY H-PLANE WAVEGUIDE JUNCTIONS BY THE BI-RME METHOD

P. Arcioni, M. Bressan, G. Conciauro and L. Perregrini

Dept. of Electronics, University of Pavia, via Ferrata 1, 27100 Pavia, ITALY

## ABSTRACT

This paper describes the extension of the BI-RME method to the determination of the generalized Y-matrix of arbitrary H-plane waveguide junctions. The method yields this matrix in the form of a pole expansion in the frequency domain. The generalized matrix is very useful in the wideband analysis of complex structures that include the junction as a building block. An example demonstrates the advantages of this extension of the BI-RME method.

## INTRODUCTION

Recently, we described and implemented in a CAD tool a very efficient algorithm (BI-RME method) for the wideband modeling of waveguide components [1], [2], [3], [4], [5]. Though, in principle, the BI-RME method can be used to analyze "en bloc" very complex circuits (e.g., multiplexers or beam forming networks), its direct use in the analysis of large components may be not convenient. In this case, as a rule, it is preferable to segment the component into building blocks and to apply the full-wave analysis only to the blocks whose frequency behavior is unknown. The building blocks must be modeled by some generalized matrix, such as the Y-matrix [6].

This paper describes the extension of the BI-RME method to the determination of the generalized Y-matrix of an arbitrarily shaped element of a rectangular waveguide circuit in the H-plane (Fig. 1). Apart from the efficiency of the BI-RME method in the analysis of the blocks, the peculiarity of yielding directly the wideband model of a block in the form of a pole expansion gives the BI-RME method the additional advantage of permitting to find the overall Y-matrix of the whole component, by a very efficient algorithm.

Work supported by ESA-ESTEC under Contract no. 10966/94/NL/NBP and by ASI under Contract no. ARS-96-190.

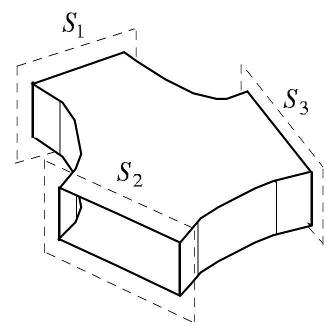


Fig. 1. An arbitrarily shaped H-plane waveguide element. Many TE$_{p0}$ modes are considered at the planes S$_m$.

This feature will be discussed in an extended version of this paper.

## THEORY

The same type of reasoning reported in [1] leads to the following wide-band representation of the generalized Y-matrix:

$$Y^{p,q}_{m,n}(\omega) = \frac{A^{p,q}_{m,n}}{j\eta k} + \frac{jk}{\eta} B^{p,q}_{m,n} + \frac{jk^3}{\eta} \sum_i \frac{C^p_{m,i} C^q_{n,i}}{\kappa_i^2(\kappa_i^2 - k^2)} \quad (1)$$

where $k = \omega\sqrt{\epsilon\mu}$, $\eta = \sqrt{\mu/\epsilon}$ and $Y^{p,q}_{m,n}$ relates the current of the TE$_{p0}$ mode on the reference plane $S_m$ (see Fig. 1) to the voltage of the TE$_{q0}$ mode on the reference plane $S_n$. In this expression $A^{p,q}_{m,n}$ and $B^{p,q}_{m,n}$ are real coefficients which determine the low-frequency behavior of $Y^{p,q}_{m,n}$; $\kappa_i$ is the the $i$-th eigenvalue of the equation (see also Fig. 2):

$$\nabla^2\psi + \kappa^2\psi = 0 \quad \text{in } S \quad (2)$$

$$\psi = 0 \quad \text{on } \partial S \quad (3)$$

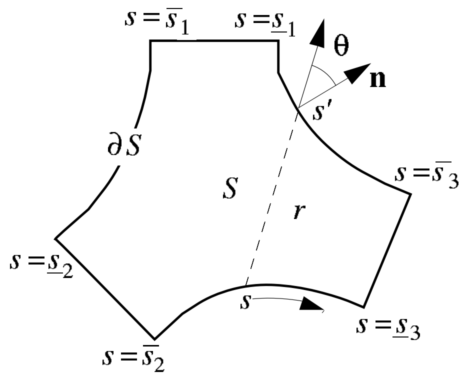


Fig. 2. The geometry of the problem.

and the coefficients $C^p_{m,i}$ are deduced from the $i$-th eigenfunction $\psi_i$ by the equation:

$$C^p_{m,i} = \frac{1}{\kappa_i}\int_{\underline{s}_m}^{\bar{s}_m} \frac{\partial\psi_i}{\partial n}\, e^p_m\, ds \tag{4}$$

$$e^p_m = \begin{cases} \sqrt{\frac{2}{\bar{s}_m-\underline{s}_m}}\,\sin\frac{p\pi(s-\underline{s}_m)}{\bar{s}_m-\underline{s}_m} & \text{in } [\underline{s}_m,\bar{s}_m] \\ 0 & \text{elsewhere} \end{cases} \tag{5}$$

where $s$ is a coordinate taken along the boundary $\partial S$, and $[\,\underline{s}_m, \bar{s}_m\,]$ is the interval spanned by the $m$-th port.

The eigensolutions of (2), (3) are determined by the BI-RME method, just as described in [1]. On the contrary, $A^{p,q}_{m,n}$ and $B^{p,q}_{m,n}$ cannot be expressed by the simple approximate formulas used in that paper, because these formulas assume that the distances between the reference planes and the discontinuities are one half cutoff-wavelength of the waveguide, at least. Of course, this assumption cannot be made for the building blocks resulting from the segmentation technique, where these distances can be arbitrarily small. Therefore, in this case $A^{p,q}_{m,n}$ and $B^{p,q}_{m,n}$ must be determined numerically. A convenient method is discussed below.

We start from the general formula

$$Y^{p,q}_{m,n} = \int_{\underline{s}_m}^{\bar{s}_m} e^p_m\, H^q_n\, ds \tag{6}$$

where $H^q_n$ is the tangential magnetic field, generated by a unit TE$_{q0}$-mode voltage applied at $S_n$, when all other voltages are zero. $H^q_n$ satisfies the boundary integral equation [7]:

$$j\eta k \oint_{\partial S} G(r) H^q_n(s')ds' = \frac{e^q_n(s)}{2} + \int_{\underline{s}_n}^{\bar{s}_n} \cos\theta \frac{\partial G(r)}{\partial r} e^q_n(s')ds' \tag{7}$$

where:

$$G(r) = \frac{\mathrm{H}^{(2)}_0(kr)}{4j} \tag{8}$$

is the free-space Green's function in two dimensions. Equation (7) determines the magnetic field for any positive value of $k$, excepting those at which the homogeneous equation has non-trivial solutions. These values are the resonance wavenumbers of the short-circuited element of Fig. 1, i.e., the eigenvalues of (2), (3). Then for any positive value of $k$ below the lowest resonance, the solution of (7) is a continuous function of $k$, and, according to (1) and (6), we expect it is of the type:

$$H^q_n = \frac{\alpha^q_n(s)}{j\eta k} + jk\frac{\beta^q_n(s)}{\eta} + O(k^3) \tag{9}$$

where $\alpha^q_n$ and $\beta^q_n$ are real functions defined on $\partial S$, related to $A^{p,q}_{m,n}$ and $B^{p,q}_{m,n}$ by the equations:

$$A^{p,q}_{m,n} = \int_{\underline{s}_m}^{\bar{s}_m} e^p_m \alpha^q_n\, ds \tag{10}$$

$$B^{p,q}_{m,n} = \int_{\underline{s}_m}^{\bar{s}_m} e^p_m \beta^q_n\, ds \tag{11}$$

Then we need a method for the determination of $\alpha^q_n$ and $\beta^q_n$.

In the Appendix we show that the free-space Green's function in (7) can be replaced by

$$G'(r) = -\frac{1}{2\pi}\ln\frac{r}{a} - \frac{1}{2\pi}\sum_{h=1}^{\infty} k^{2h}\frac{(-1)^h}{(h!)^2} \cdot \left(\frac{r}{2}\right)^{2h}\left(\ln\frac{r}{a} - 1 - \frac{1}{2} - \cdots - \frac{1}{h}\right) \tag{12}$$

where $a$ is an arbitrary distance. This replacement has two advantages: *i* - the new Green's function is real, reflecting the standing-wave behavior of the field in a closed and lossless region; *ii* - it has the form of a power series in $k$, like (9). This last feature permits to derive the following equations, obtained by substituting (9) into (7), replacing $G(r)$ by (12), and equating terms containing equal powers of $k$ on both sides of

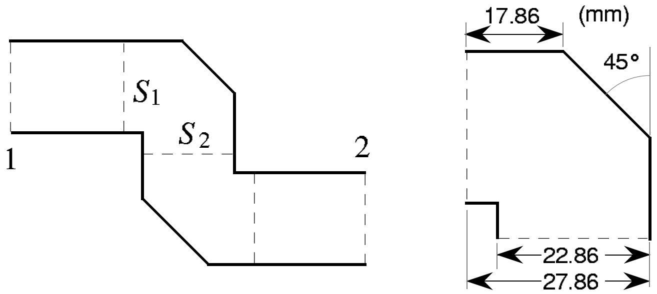

Fig. 3. The H-plane double bend used to test the algorithm.

the integral equation:

$$\oint_{\partial S} \alpha_n^q(s') \ln\frac{r}{a}\, ds' = -\pi \epsilon_n^q(s) + \int_{\underline{s}_n}^{\bar{s}_n} \frac{\cos\theta}{r}\, \epsilon_n^q(s') ds' \qquad (13)$$

$$\oint_{\partial S} \beta_n^q(s') \ln\frac{r}{a}\, ds' = \oint_{\partial S} \alpha_n^q(s') \frac{r^2}{4}\left(\ln\frac{r}{a} - 1\right) ds' + \int_{\underline{s}_n}^{\bar{s}_n} \epsilon_n^q(s')\, \frac{r\cos\theta}{2}\left(\frac{1}{2} - \ln\frac{r}{a}\right) ds' \qquad (14)$$

Solving these equations we obtain the functions $\alpha_n^q$ and $\beta_n^q$, that permit the calculation of $A_{m,n}^{p,q}$ and $B_{m,n}^{p,q}$ by (10), (11).

## NUMERICAL IMPLEMENTATION

Functions $\alpha_n^q$ and $\beta_n^q$ are approximated by:

$$\alpha_n^q(s) = \sum_{k=1}^{K} x_{nk}^q f_k(s) \qquad \beta_n^q(s) = \sum_{k=1}^{K} y_{nk}^q f_k(s) \qquad (15)$$

where $\{f_k\}$ is a set of basis functions defined on $\partial S$, and $x_{nk}^q$, $y_{nk}^q$ are unknown coefficients. Using the Galerkin's method, (13) and (14) are converted into the following matrix equations:

$$\mathbf{M}\mathbf{x}_n^q = \mathbf{u}_n^q \qquad (16)$$

$$\mathbf{M}\mathbf{y}_n^q = \mathbf{N}\mathbf{x}_n^q + \mathbf{v}_n^q \qquad (17)$$

where: $\mathbf{x}_n^q$, $\mathbf{y}_n^q$ are the vectors of the coefficients $x_{nk}^q$, $y_{nk}^q$; $\mathbf{M}$, $\mathbf{N}$ are $K \times K$ matrices and $\mathbf{u}_n^q$ and $\mathbf{v}_n^q$ are $K$-dimensional vectors, defined as:

$$M_{h,k} = \oint_{\partial S}\oint_{\partial S} f_h(s)\, f_k(s') \ln\frac{r}{a}\, ds\, ds'$$

$$N_{h,k} = \oint_{\partial S}\oint_{\partial S} f_h(s)\, f_k(s') \frac{r^2}{4}\left(\ln\frac{r}{a} - 1\right) ds\, ds'$$

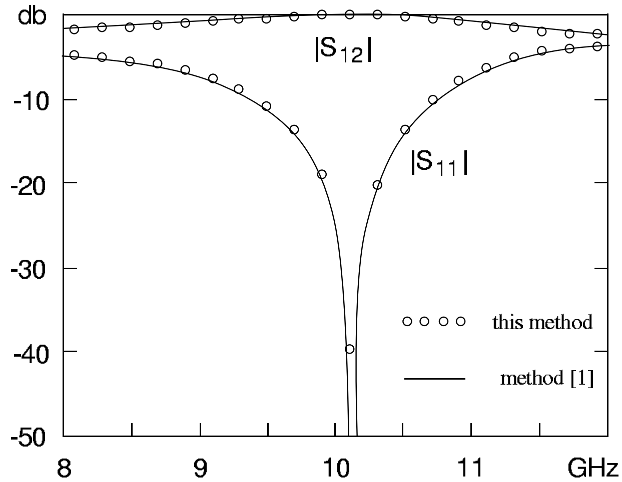

Fig. 4. Amplitude of the S-parameters of the junction of Fig. 3.

$$u_{n,k}^q = \oint_{\partial S} f_k(s) \int_{\underline{s}_n}^{\bar{s}_n} \frac{\cos\theta}{r}\, \epsilon_n^q(s')\, ds\, ds' - \pi \int_{\underline{s}_n}^{\bar{s}_n} f_k(s)\, \epsilon_n^q(s)\, ds$$

$$v_{n,k}^q = \oint_{\partial S} f_k(s) \int_{\underline{s}_n}^{\bar{s}_n} \frac{r\cos\theta}{2} \cdot \left(\frac{1}{2} - \ln\frac{r}{a}\right) \epsilon_n^q(s')\, ds\, ds'$$

Due to (10), (11), from the solution of (16) and (17), we deduce:

$$A_{m,n}^{p,q} = \mathbf{w}_m^p \mathbf{x}_n^q \qquad B_{m,n}^{p,q} = \mathbf{w}_m^p \mathbf{y}_n^q$$

where $\mathbf{w}_m^p$ is the row-vector defined as:

$$w_{m,h}^p = \int_{\underline{s}_m}^{\bar{s}_m} \epsilon_m^p f_h\, ds \qquad h = 1, 2, \ldots, K$$

Incidentally, we note that many elements of the matrix $\mathbf{M}$ are available as by-products of the algorithm used to find the eigensolutions of (2), (3).

## VALIDATION OF THE ALGORITHM

To validate the algorithm, we analyzed the WR-90 double bend of Fig. 3 by the segmentation method, calculating the generalized Y-matrix of each bend by the described procedure. Five modes were considered at the reference planes $S_1$, $S_2$. The boundary of each bend was divided into 46 segments and a set of 46

0-7803-4603-6/97/$5.00 (c) IEEE

rectangular pulse base functions were used in the approximations (15). The Y-matrix of the cascade of the two bends was used to calculate the scattering parameters relating the $TE_{10}$ wave amplitudes at the ports 1 and 2 (dots in Fig. 4). For comparison, the double bend was analyzed "en bloc" by the method [1], obtaining nearly the same results (continuous lines). Though the computation of the coefficients $A^{p,q}_{m,n}$ and $B^{p,q}_{m,n}$ has been not yet optimized with respect to the CPU time, the analysis by the generalized Y-matrix is much faster than the other (about 20 sec against 120 sec, on a Sun Sparcstation 10).

## CONCLUSIONS

The described procedure shows how the BI-RME algorithm can be extended to determine the generalized Y-matrix of arbitrarily shaped H-plane waveguide building blocks. The numerical example confirms the advantage of using the BI-RME approach together with the segmentation method, to reduce the CPU time.

## APPENDIX

From the Green's second identity we obtain:

$$\int_S \left( E\nabla^2 \mathrm{J}_0(kr) - \mathrm{J}_0(kr)\nabla^2 E \right) dS = \oint_{\partial S} \left( E \frac{\partial \mathrm{J}_0(kr)}{\partial n} - \mathrm{J}_0(kr)\frac{\partial E}{\partial n} \right) ds \qquad (18)$$

where $E$ and $\mathrm{J}_0$ denote the electric field and the Bessel function of the first kind and zero order, respectively. The integral on $S$ is zero because:

$$\nabla^2 \mathrm{J}_0(kr) + k^2 J_0(kr) = 0 \qquad \nabla^2 E + k^2 E = 0 \qquad \text{in } S$$

On the other hand, on the boundary $\partial S$ we have:

$$\frac{\partial E}{\partial n} = jk\eta H_n^q \qquad E = \epsilon_n^q$$

$$\frac{\partial J_0(kr)}{\partial n} = \vec{n} \cdot \nabla J_0(kr) = \frac{\partial J_0(kr)}{\partial r} \cos\theta$$

and (18) can be rewritten as:

$$j\eta k \oint_{\partial S} J_0(kr)\, H_n^q(s')\, ds' = \int_{\underline{s}_n}^{\overline{s}_n} \cos\theta\, \frac{\partial J_0(kr)}{\partial r}\, \epsilon_n^q(s')\, ds'$$

Therefore, replacing in (7) the Green's function (8) by:

$$G'(r) = \frac{\mathrm{H}_0^{(2)}(kr)}{4j} + CJ_0(kr)$$

($C$ = arbitrary constant), equation (7) remains valid. Using:

$$C = -\frac{1}{4j} + \frac{1}{2\pi}\left(\gamma + \ln\frac{ka}{2}\right)$$

where $\gamma$ is the Euler's constant and $a$ is an arbitrary distance, we have:

$$G'(r) = -\frac{1}{4}\left[\mathrm{N}_0(kr) - \frac{2}{\pi}\left(\gamma + \ln\frac{ka}{2}\right)\mathrm{J}_0(kr)\right] = \frac{1}{2\pi}\sum_{h=1}^{\infty}\frac{(-1)^h}{(h!)^2}\left(\frac{kr}{2}\right)^{2h}\left(1 + \frac{1}{2} + \ldots \frac{1}{h}\right) - \frac{1}{2\pi}\mathrm{J}_0(kr)\ln\frac{r}{a}$$

from which we obtain (12) by power-expanding $\mathrm{J}_0$.

## References


[1] G. Conciauro, P. Arcioni, M. Bressan, L. Perregrini, "Wideband Modeling of Arbitrarily Shaped H-Plane Components by the Boundary Integral - Resonant Mode Expansion Method", *IEEE Trans. on Microwave Theory Tech.*, vol. MTT-44, no. 7, July 1996, pp. 1057–1066.

[2] P. Arcioni, M. Bressan, G. Conciauro, L. Perregrini, "Wideband Modeling of Arbitrarily Shaped E-Plane Components by the Boundary Integral - Resonant Mode Expansion Method", *IEEE Trans. on Microwave Theory Tech.*, vol. MTT-44, no. 11, Nov. 1996, pp. 2083–2092.

[3] P. Arcioni, M. Bressan, G. Conciauro, L. Perregrini, "A Fast Algorithm for the Wideband Analysis of 3-D Waveguide Junctions", Proc. of the Second Int. Conf. on Computation in Electromagnetics, Nottingham, UK, April 12-14, 1994, pp. 311-314.

[4] P. Arcioni, M. Bressan, G. Conciauro, L. Perregrini, "Fast Analysis of Waveguide Components for Antenna Feed Systems", Proc. of PIERS 94, Noordwijk, The Netherlands, July 11-15, 1994, pp. 1458–1461.

[5] P. Arcioni, M. Bressan, G. Conciauro, L. Perregrini, G. Gatti "ANAPLAN-W: a CAD Tool for E/H-Plane Waveguide Circuits", *ESA - Preparing for the Future*, vol. 6, n.1, March 1996, pp. 12–13.

[6] F. Alessandri, G. Bartolucci, R. Sorrentino, "Admittance Matrix Formulation of Waveguide Discontinuity Problems: Computer Aided Design of Branch Guide Directional Couplers", *IEEE Trans. Microwave Theory Tech.*, vol. MTT-36, Feb. 1988, pp. 394–403.

[7] T. Okoshi, "Planar Circuits for Microwaves and Lightwaves", Springer-Verlag, Berlin, Germany,1985, Sec. 3.2.